Sequential Exposure to Carbon Nanotubes and Bacteria Enhances Pulmonary Inflammation and Infectivity

Anna A. Shvedova[1], James P. Fabisiak[2], Elena R. Kisin[1], Ashley R. Murray[1], Jenny R. Roberts[1], Yulia Y. Tyurina[2], James M. Antonini[1], Wei Hong Feng[2], Choudari Kommineni[1], Jeffrey Reynolds[1], Aaron Barchowsky[2], Vince Castranova[1], and Valerian E. Kagan[2]

[1]Pathology/Physiology Research Branch, HELD, National Institute for Occupational Safety and Health, Morgantown, West Virginia; and [2]Departments of Environmental and Occupational Health and Pharmacology, Center for Free Radical and Antioxidant Health, Graduate School of Public Health, University of Pittsburgh, Pittsburgh, Pennsylvania

Carbon nanotubes (CNT), with their applications in industry and medicine, may lead to new risks to human health. CNT induce a robust pulmonary inflammation and oxidative stress in rodents. Realistic exposures to CNT may occur in conjunction with other pathogenic impacts (microbial infections) and trigger enhanced responses. We evaluated interactions between pharyngeal aspiration of single-walled CNT (SWCNT) and bacterial pulmonary infection of C57BL/6 mice with *Listeria monocytogenes* (LM). Mice were given SWCNT (0, 10, and 40 μg/mouse) and 3 days later were exposed to LM (10^3 bacteria/mouse). Sequential exposure to SWCNT/LM amplified lung inflammation and collagen formation. Despite this robust inflammatory response, SWCNT pre-exposure significantly decreased the pulmonary clearance of LM-exposed mice measured 3 to 7 days after microbial infection versus PBS/LM-treated mice. Decreased bacterial clearance in SWCNT-pre-exposed mice was associated with decreased phagocytosis of bacteria by macrophages and a decrease in nitric oxide production by these phagocytes. Pre-incubation of naïve alveolar macrophages with SWCNT *in vitro* also resulted in decreased nitric oxide generation and suppressed phagocytizing activity toward LM. Failure of SWCNT-exposed mice to clear LM led to a continued elevation in nearly all major chemokines and acute phase cytokines into the later course of infection. In SWCNT/LM-exposed mice, bronchoalveolar lavage neutrophils, alveolar macrophages, and lymphocytes, as well as lactate dehydrogenase level, were increased compared with mice exposed to SWCNT or LM alone. In conclusion, enhanced acute inflammation and pulmonary injury with delayed bacterial clearance after SWCNT exposure may lead to increased susceptibility to lung infection in exposed populations.

Keywords: nanoparticles; infection; inflammation; lung disease; pulmonary injury

CLINICAL RELEVANCE

Exposure to carbon nanotubes and infection induces unusual responses in which both mutually enhance inflammation and depress bacterial clearance. Nanotubes may increase susceptibility to lung infection in exposed populations.

Nanotechnology, with its increasingly sophisticated ability to manipulate matter at the nanoscale, has already yielded new materials, products, and devices that demonstrate new and unusual behavior and are believed to be beneficial for many industries, as well as for medicine (1). Among different types of nanomaterials, carbon nanotubes (CNT), particularly single-walled (SW)CNT, have already found numerous industrial applications. There are growing concerns, however, that the same attributes that make nanomaterials technologically attractive may lead to new risks to human health, particularly after their irrational or unjustified use (2). The results of several *in vivo* studies on rodents demonstrated that CNT are capable of inducing inflammation, granulomas, fibrosis, and biochemical/toxicological changes in the lungs (3). Moreover, there are complex interactions between the pathophysiologic mechanisms—inflammatory response and oxidative stress—that can synergistically amplify each other to cause enhanced pulmonary toxicity during exposure to SWCNT (4).

Inflammation may arise through multiple factors, the most notable being a natural response to microbial infection. Therefore, it is possible that toxic effects of SWCNT will modify or be modified by microbial infection–induced inflammation. This potential interaction will be important for occupational exposures to nanoparticles as well as in nanomedicine, where development of novel approaches for treatment of invasive infections encompasses new delivery systems including nanoparticles/nanospheres that can substantially modulate the pharmacokinetics of existing compounds, and may also be useful to enhance the delivery of agents to sites of infection (5). For example, adherence of microorganisms to cells represents the initial step in the establishment of infection and, accordingly, modification of this step using nanoparticles with bioadhesive properties represents a method by which the incidence of infection may be manipulated (6).

The lung is the prime target for SWCNT toxicity, as they can be inhaled during technologic processing and use (1). Therefore, in the current work, we employed the model of pharyngeal SWCNT aspiration and evaluated the effect of this exposure on bacterial clearance, cytokine/chemokine production, and collagen deposition in mice subsequently infected with *Listeria monocytogenes* (LM). We report that SWCNT significantly decreased the pulmonary clearance of LM, resulting in a continued elevation in nearly all major chemokines and acute phase cytokines into the later course of infection. Significantly increased numbers of neutrophils (PMNs), alveolar macrophages (AM), and lymphocytes, as well as elevated lactate dehydrogenase (LDH) activity, were found in SWCNT and LM co-exposed mice as compared with those mice exposed to either stimulus alone. Notably, the SWCNT-dependent persistence of bacteria was accompanied by enhanced adaptive immune responses as evidenced by increased accumulation of lymphocytes, as well as lymphocyte-derived cytokines such as IFN-γ and IL-17. Decreased bacterial clearance in SWCNT-pre-exposed mice was also associated with decreased phagocytosis of bacteria by AMs and a decrease in nitric oxide production by these phagocytes.

(*Received in original form July 3, 2007 and in final form November 13, 2007*)

Disclaimer: The findings and conclusions in this report are those of the authors and do not necessarily represent the views of the National Institute for Occupational Safety and Health.

This study was supported by NIOSH OH008282, National Institutes of Health HL70755 (to V.E.K.) and RO1-ES-011986 (to J.P.F.), NORA 927000Y, and the Human Frontier Science Program.

Correspondence and requests for reprints should be addressed to Anna A. Shvedova, Ph.D., NIOSH, PPRB, 1095 Willowdale Rd., Morgantown, WV 26505. E-mail: ats1@cdc.gov

Am J Respir Cell Mol Biol Vol 38. pp 579–590, 2008
Originally Published in Press as DOI: 10.1165/rcmb.2007-0255OC on December 20, 2007
Internet address: www.atsjournals.org

MATERIALS AND METHODS

Animals

Specific pathogen–free adult female C57BL/6 mice (7–8 wk old) were supplied by Jackson Labs (Bar Harbor, ME) and weighed 20.3 ± 0.21 g at time of use. Animals were individually housed in the American Association for Accreditation of Laboratory Animal Care–approved National Institute for Occupational Safety and Health (NIOSH) animal facilities. Mice were acclimated in microisolator cages for 1 wk before use. Autoclaved Beta Chip bedding (Northeastern Products, Warrensburg, NY) was changed weekly. Animals were supplied with water and food (Harlan Teklad, 7913, NIH-31 Modified Mouse/Rat Diet, Irradiated; Harlan Teklad, Madison, WI) and housed under controlled light, temperature, and humidity conditions. Experiments were conducted under a protocol approved by the Animal Care and Use Committee of NIOSH.

Experimental Design

Experimental protocol of pharyngeal aspiration of C57BL/6 mice with SWCNT and/or LM is presented in Figure 1A. Animals were pre-treated with SWCNT (10 μg/mouse or 40 μg/mouse; 60 μl) or PBS (60 μl) via pharyngeal aspiration on Day 0. At Day 3, the animals were inoculated by pharyngeal aspiration with LM (10^3 bacteria; 40 μl). Uninfected animals in each treatment group received saline on Day 3. Animals were killed on Days 3, 6, 8, and 10 of experiment. As a result, the six experimental groups were: PBS/PBS—uninfected animals pre-exposed to PBS; SWCNT (10 μg/mouse)/PBS—uninfected animals that had received a low dose of SWCNT; SWCNT (40 μg/mouse)/PBS—uninfected animals that had received a high dose of SWCNT; PBS/LM—infected animals pre-exposed to PBS; SWCNT (10 μg/mouse)/LM—infected animals pre-exposed to a low dose of SWCNT; SWCNT (40 μg/mouse)/LM—infected animals pre-exposed to a high dose of SWCNT. Inflammation was evaluated by total cell counts, cell differentials, and accumulation of cytokines (acute phase reactants, chemotactic factors, and immune modulators) in the bronchoalveolar lavage (BAL) fluid. Pulmonary toxicity was assessed by elevation of LDH level in acellular BAL fluid. Fibrogenic responses to exposed materials were assessed by histopathologic evaluation of lung tissue and collagen deposition. Lung defense responses were measured by decreased bacterial clearance (*L. monocytogenes*) in lung of inoculated mice.

Particles

SWCNT (CNI, Houston, TX) produced by the high-pressure CO disproportionation (HiPco) process (7), employing CO in a continuous-flow gas phase as the carbon feedstock and $Fe(CO)_5$ as the iron-containing catalyst precursor and purified by acid treatment to remove metal contaminates (8), were used in the study. Chemical analysis of total elemental carbon and trace metal (iron) in SWCNT was performed at the Chemical Exposure and Monitoring Branch (Division of Applied Research and Technology/NIOSH, Cincinnati, OH). Elemental carbon in SWCNT (HiPco) was assessed according to the NIOSH Manual of Analytical Methods (NMAM) (9), whereas metal content (iron) was analyzed by nitric acid dissolution and inductively coupled plasma-atomic emission spectrometry (ICP-AES). Analytical analysis performed by NMAM 5040 and ICP-AES revealed that SWCNT comprises 99.7% (wt) elemental carbon and 0.23% (wt) iron. For purity assessment of HiPco SWCNT, we used several standard analytical techniques, including thermo-gravimetric analysis with differential scanning colorimetry (TGA-DSC), thermo-programming oxidation (TPO), and Raman and near-infrared (NIR) spectroscopy (10, 11). Comparative analytical data obtained by TGA-DSC, TPO, NIR, and Raman spectroscopy revealed that more than 99% of carbon content in the SWCNT HiPco product was accountable in a carbon nanotube morphology. Purified suspended HiPco SWCNT (8) were used in the study (0.7 mg/ml). The mean diameter and surface area of SWCNT were 1 to 4 nm and 1,040 m^2/g, respectively. The length of the individual SWCNT is approximately 1 to 3 μm. Surface area was determined by Brunauer, Emmett, and Teller analysis, and diameter and length were measured by transmission electron microscopy (TEM).

Particle or LM Instillation

Mouse pharyngeal aspiration was used for SWCNT or bacteria administration. In brief, after anesthesia with a mixture of ketamine and xylazine (Phoenix, St. Joseph, MO) (62.5 and 2.5 mg/kg subcutaneous in the abdominal area), the mouse was placed on a board in a near-vertical position, and the tongue was gently extended with lined forceps. A suspension of SWCNT (0, 10, and 40 μg/mouse; 60 μl in saline) or LM (10^3 bacteria; 40 μl in saline) was placed posterior in the throat, and the tongue was held until the suspension was aspirated into the lungs. Particles were sterilized before administration. All mice in particle, bacteria, and PBS groups survived this exposure procedure. This technique provides good distribution of particles widely disseminated in a peribronchiolar pattern within the alveolar region (12). All animals recovered easily after anesthesia with no behavioral or negative health outcomes.

Bronchoalveolar Lavage

Mice were weighed and killed with intraperitoneal injection of pentobarbital sodium (> 100 mg/kg; Fort Dodge Animal Health, Fort Dodge, IA). The trachea was cannulated with a blunted 22-gauge needle, and BAL was performed with cold sterile Ca^{2+} and Mg^{2+}-free PBS at a volume of 0.9 ml for first lavage (kept separate) and 1.0 ml for subsequent lavages. Approximately 5 ml of BAL fluid per mouse were collected and pooled in sterile centrifuge tubes. Pooled BAL cells were washed in Ca^{2+} and Mg^{2+}-free PBS by alternate centrifugation ($800 \times g$ for 10 min at 4°C) and resuspension. Cell-free first-fraction BAL aliquots were frozen and kept until processed.

BAL Cell Counting and Differentials

The degree of inflammatory response induced by the pharyngeally aspirated particles was estimated by the total cells, macrophages, PMNs, and lymphocytes recruited into the mouse lungs and recovered in the BAL fluid. Cell counts were performed with an electronic cell counter equipped with a cell sizing attachment (Coulter model Multisizer II with a 256C channelizer; Coulter Electronics, Hialeah, FL). Alveolar macrophages, neutrophils, and lymphocytes were identified by their characteristic cell shape in cytospin preparations stained with a Hema-3 kit (Fisher Scientific, Pittsburgh, PA), and differential counts of BAL cells were performed. Three hundred cells per slide were counted.

Lung Fixation and Histopathology

Lung tissues were prepared for histologic analysis under standard conditions. Preservation of the lung was achieved by vascular perfusion of a fixative. This method of fixation was chosen to prevent possible disturbances of the airspace distribution of deposited materials while maintaining physiologic inflation levels comparable to that of the end-expiratory volume. This was performed using protocols previously employed to study pulmonary effects of SWCNT (13, 14). Briefly, the animal was anesthetized (ketamine/xylazine 50 and 2 mg/kg, respectively) by subcutaneous injection in the abdomen, the trachea was cannulated, and laparotomy was performed. Mice were then killed by exsanguination. The pulmonary artery was cannulated via the ventricle and an outflow cannula inserted into the left atrium. In quick succession, the tracheal cannula was connected to a 5 cm H_2O pressure source, and clearing solution (saline with 100 U/ml heparin, 350 mosM sucrose) was perfused to clear blood from the lungs. The perfusate was switched to fixative consisting of 2% glutaraldehyde and 1% formaldehyde and 1% tannic acid with sucrose as an osmotic buffer. Tannic acid was included to produce an electron-dense staining of connective tissue fibers and to assist in preservation of lipid structures in the lungs. Fixed lung volume was measured by water displacement (15). Coronal sections were cut from the lungs, and the lungs were embedded in paraffin, sectioned at a thickness of 5 μm with an HM 320 rotary microtome (Carl Zeiss, Thornwood, NY). Lung sections were stained with hematoxylin and eosin. Airways, terminal bronchioles, and the lung parenchyma were examined microscopically for the presence of cellular changes and inflammation. To quantitatively determine the magnitude of inflammatory response in the lungs of mice, 10 random sections of each sample tissue were assessed for neutrophil influx.

Lung Collagen Measurements

Total lung collagen content was determined by quantifying total soluble collagen using the Sircol Collagen Assay kit (Accurate Chemical and Scientific Corporation, Westbury, NY). Briefly, whole lungs were homogenized in 0.7 ml of 0.5 M acetic acid containing pepsin with 1:10 ratio of pepsin/tissue wet weight. Each sample was stirred vigorously for 24 hours at 4°C, centrifuged, and 200 μl of supernatant was assayed according to

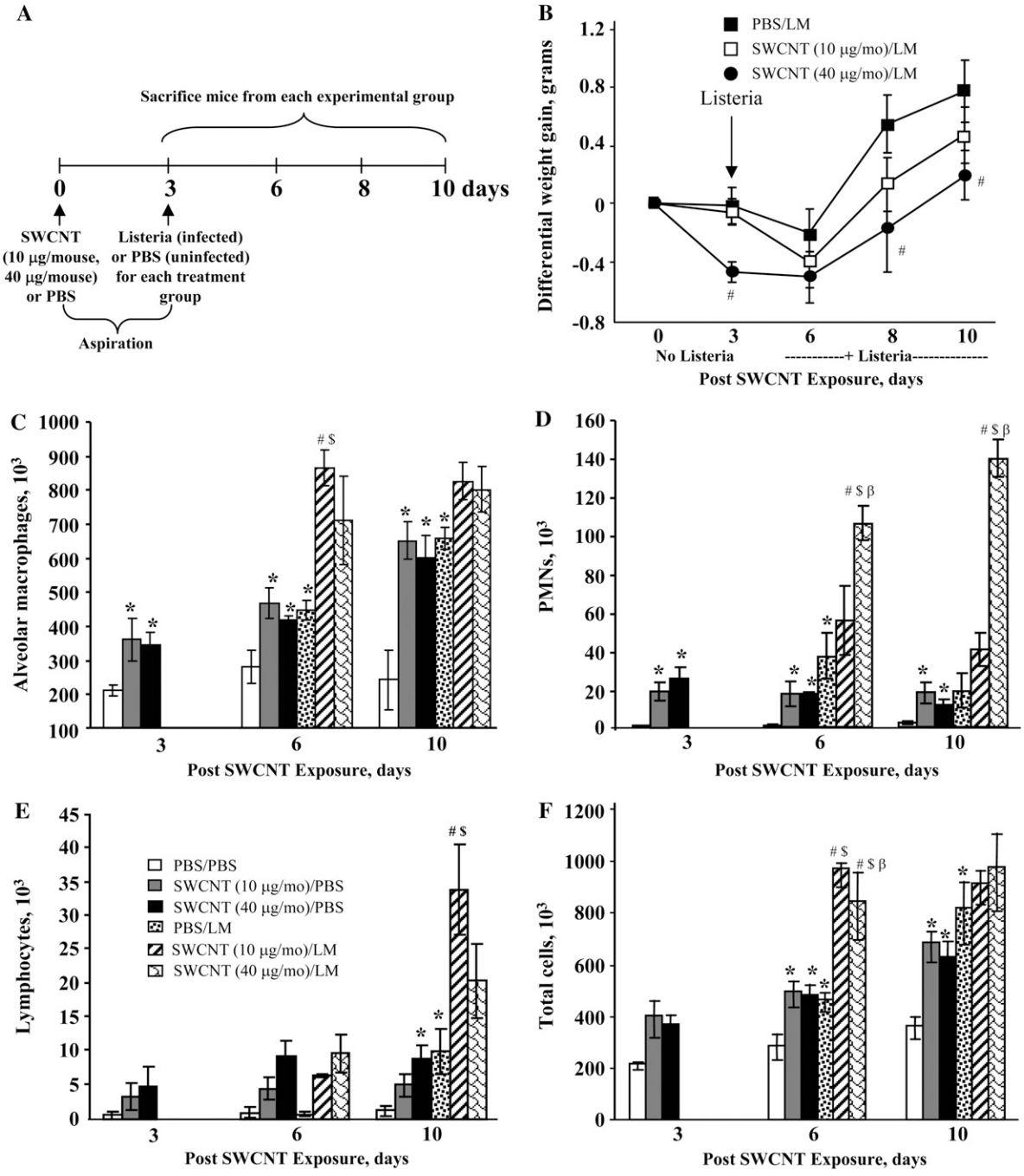

Figure 1. (*A*) Experimental protocol of pharyngeal aspiration of C57BL/6 mice with single-walled carbon nanotubes (SWCNT) and/or *Listeria monocytogenes* (LM). (*B*) Differential weight gain of C57BL/6 mice pre-exposed to PBS (*solid squares*), 10 μg/mouse SWCNT (*open squares*), or 40 μg/mouse SWCNT (*circles*) 3 days before inoculation with LM. Data represent mean ± SEM obtained from six mice per group. (*C–F*) Cell profile of BAL samples from C57BL/6 mice after pharyngeal aspiration with SWCNT and/or LM: *C*, alveolar macrophages; *D*, PMNs; *E*, lymphocytes; *F*, total cells. *Open bars* represent uninfected animals pre-exposed to PBS (PBS/PBS group); *gray bars* represent uninfected animals that had received a low dose of SWCNT (SWCNT, 10 μg/mouse/PBS group); *solid bars* represent uninfected animals that had received a high dose of SWCNT (SWCNT, 40 μg/mouse/PBS group); *dotted bars* represent infected animals pre-treated with PBS (PBS/LM group); *diagonal bars* represent infected animals that had received a low dose of SWCNT (SWCNT, 10 μg/mouse/LM group); *brick bars* represent infected animals that had received a high dose of SWCNT (SWCNT, 40 μg/mouse/LM group). $^{*}P < 0.05$ versus PBS/PBS control group; $^{\#}P < 0.05$ versus PBS/LM-treated animals; $^{\$}P < 0.05$ versus SWCNT, 10 μg/mouse/PBS-treated mice; $^{\beta}P < 0.05$ versus SWCNT, 40 μg/mouse/PBS-treated mice.

the manufacturer's instructions (Accurate Chemical and Scientific Corporation, Westbury, NY).

Measurements of Cytokines

Multicytokine array analysis was performed using Luminex-based Bioplex system (Bio-Rad, Hercules, CA) according to the manufacturer's instructions. Briefly, anti-cytokine/chemokine conjugated beads were added to individual wells of a 96-well filter plate and adhered using vacuum filtration. After washing, 50 μl of prediluted standards or BAL supernatants were added and incubated for 30 minutes at room temperature with rotation at 300 rpm. Thereafter, the filter plate was washed and 25 μl of pre-diluted multiplex detection antibody added

and the filter plate again incubated as described above. After washing, 50 μl of pre-diluted streptavidin-conjugated phycoerythrin was added, and the filter plate shaken at 300 rpm for 10 minutes. After washing, 125 μl of Bio-Plex assay buffer was added to each well and the filter plate plate analyzed using the Bio-Plex Protein Array System. The concentrations of each cytokine and chemokine were determined using Bio-Plex Manager Version 3.0 software and data expressed as pg/ml.

LDH Activity in BAL Fluid

The activity of LDH in the BAL supernatant was assayed spectrophotometrically by monitoring the reduction of nicotinamide adenine dinucleotide at 340 nm in the presence of lactate (Pointe Scientific, Lincoln Park, MI).

Measurements of Reactive Oxygen Species

To estimate total lung oxidant burden, luminol-dependent chemiluminescence (CL) was performed on BAL cells as a measure of the light generated by the production of reactive oxygen species (ROS) using a Berthold LB953 luminometer (Wallace Inc., Gaithersburg, MD) as described previously (16). Phorbol 12-myristate 13-acetate (PMA) (10 μM), a soluble stimulant of total BAL phagocytes, was added to the assay immediately before CL measurement to determine the contribution of BAL cells to the overall production of ROS in the lungs of the mice. Measurement of CL was recorded for 15 minutes at 37°C, and the integral of counts per minute (cpm) per 10^5 cells versus time was calculated. CL was calculated as the cpm of the stimulated cells minus the cpm of the corresponding resting cells, and the value was normalized to total number of BAL cells for PMA-stimulated CL.

Pulmonary Bacterial Inoculation and Clearance

L. monocytogenes (strain 10403S, serotype 1) was cultured overnight in brain-heart infusion broth at 37°C in a shaking incubator. After incubation, the bacterial concentration was determined at an optical density of 600 nm and diluted with sterile saline to a concentration of 1×10^3 LM in 40 μl of sterile saline. In a previous pilot study, this bacterial dose gave a uniform infection, and did not have any effect on mortality compared with naïve C57BL/6 mice. At 3, 5, and 7 days after LM inoculation, which corresponded to 6, 8, and 10 days after SWCNT aspiration, the lungs were removed from the mice of each treatment group. The excised whole lung tissues were suspended in 5 ml of sterile water, homogenized, and cultured on brain-heart infusion agar plates. The number of viable colony-forming units (CFU) was counted after an overnight incubation at 37°C.

Ex Vivo Experiment

Mice were pharyngeally aspirated with SWCNT (0, 10, or 40 μg/mouse) and AMs were obtained on Day 3 after exposure. The recovered AMs were allowed to adhere to an 8-well chamber slide (0.5×10^5 cells/well) for 1 hour at 37°C in RMPI 1640 media (Sigma Chemical Co., St Louis, MO) with 10% fetal bovine serum (FBS).

In Vitro Experiment

AMs were isolated from naive C57BL/6 mice. The recovered AMs were allowed to adhere to an 8-well chamber slide (0.5×10^5 cells/well) for 1 hour at 37°C in RMPI 1640 media (Sigma Chemical Co.) with 10% FBS. The adherent cells were pre-exposed to SWCNT (0, 90, or 240 μg/ml) for 1 hour at 37°C.

Assay of Macrophage Phagocytizing Activity

To identify the ability of macrophages from SWCNT-exposed animals to phagocytize LM, the adherent AMs (0.5×10^5 cells/well) in 8-well chamber slides were exposed to *L. monocytogenes* (1×10^6 bacteria per well) pre-stained with Cell Tracker Green (2 μM) as described previously (17). Macrophages were fixed with 2% paraformaldehyde, stained with Nile Red (62.8 μM) for 15 minutes, and analyzed using fluorescence microscopy. Phagocytosis was measured by counting Cell Tracker Green positive macrophages. Three hundred macrophages per sample were counted.

NO Production by AMs

Intracellular production of nitric oxide was assessed using a 4,5-diaminofluorescein diacetate (DAF-2DA; Calbiochem, San Diego, CA) oxidation assay (18). 4,5-diaminofluoresceine (DAF-2) in the cells specifically reacts with NO and yields fluorescent DAF-2–Triazole (DAF-2T) (19). AMs (0.5×10^5/well) treated with SWCNT *in vivo* (10 and 40 μg/mouse) or *in vitro* (90 and 240 μg/ml, for 1 h), were pre-incubated with DAF-2DA (2 μM for 1 h at 37°C). The macrophages were then incubated with LM (1×10^6 bacteria/well) for 1 hour at 37°C. For fluorescence microscopy, cells were washed with PBS and fixed/stained with Hoechst 33342 (2 μg/ml; Molecular Probes, Invitrogen, Carlsbad, CA) in 2% paraformaldehyde for 1 hour. Treated cells were examined under a Nikon ECLIPSE TE 200 fluorescence microscope (Tokyo, Japan) equipped with a digital Hamamatsu charge-coupled device camera (C4742–95–12NBR) and analyzed using the MetaImaging Series software version 4.6 (Universal Imaging Corp., Downingtown, PA). Three hundred macrophages per sample were counted.

Statistical Analysis

Results were compared by one-way ANOVA using the all pairwise multiple comparison procedures (Holm-Sidak method) or Dunnett's Multiple Comparisons to Control, and Student's unpaired *t* test with Welch's correction for unequal variances. All results are presented as means ± SE. *P* values of < 0.05 were considered to be statistically significant.

RESULTS

Body Weight

Body weight was assessed throughout the experimental schedule to monitor the general health of the animals exposed to SWCNT and/or LM (Figure 1B). Pharyngeal aspiration of SWCNT at the dose of 40 μg/mouse caused significant reduction of weight compared with PBS-treated controls 3 days after the exposure. The significant differences in decreased body weight were also observed on Days 8 and 10 of the experiment after the combined exposure to SWCNT (high dose) plus LM. At a lower dose of SWCNT (10 μg/mouse) followed by LM inoculation, no significant changes in body weight were detected compared with infected mice pre-treated with PBS.

Characterization of Inflammatory Response

Inflammatory cells. SWCNTs exposure alone increased the number of PMNs and AMs on Day 3 of the experiment and the total number of BAL cells on Exposure Days 6 and 10 (Figures 1C and 1D). Exposure to LM alone increased the BAL content of PMNs and AMs by Day 6 and lymphocytes by Day 10. Co-exposure to SWCNT and LM resulted in robust total accumulation of AMs and PMNs by Day 6 and PMNs and lymphocytes by Day 10 of the experiment compared with separate exposures of LM or SWCNT.

Cytotoxicity. In agreement with our previous results, SWCNT induced cell damage in the lung of exposed C57BL/6 mice. On Day 3, the exposure to nanotubes caused substantial release of LDH, which tended to return toward normal 10 days after exposure (Figure 2A). LM alone did not cause cytotoxicity. However, the cytotoxic effects were enhanced in the SWCNT/LM groups on Day 6 of the experiment. By Day 10, this augmented LDH release was observed only at the higher SWCNT dose combined with LM.

Histopathologic evaluation. Histopathologic analysis was performed on lungs from the treatment groups, and representative micrographs from each group at Day 10 after SWCNT aspiration are depicted in Figures 2C–2F). Pneumonitis, characterized by a peribronchiolar accumulation of PMNs and the appearance of granulomatous lesions, was observed throughout the lungs for the group treated with SWCNT alone (Figure 2D). LM exposure alone (Figure 2E) showed characteristics of pulmonary infection exhibited by a mixed inflammatory cell infiltrate (mononuclear cells and PMNs). For the SWCNT

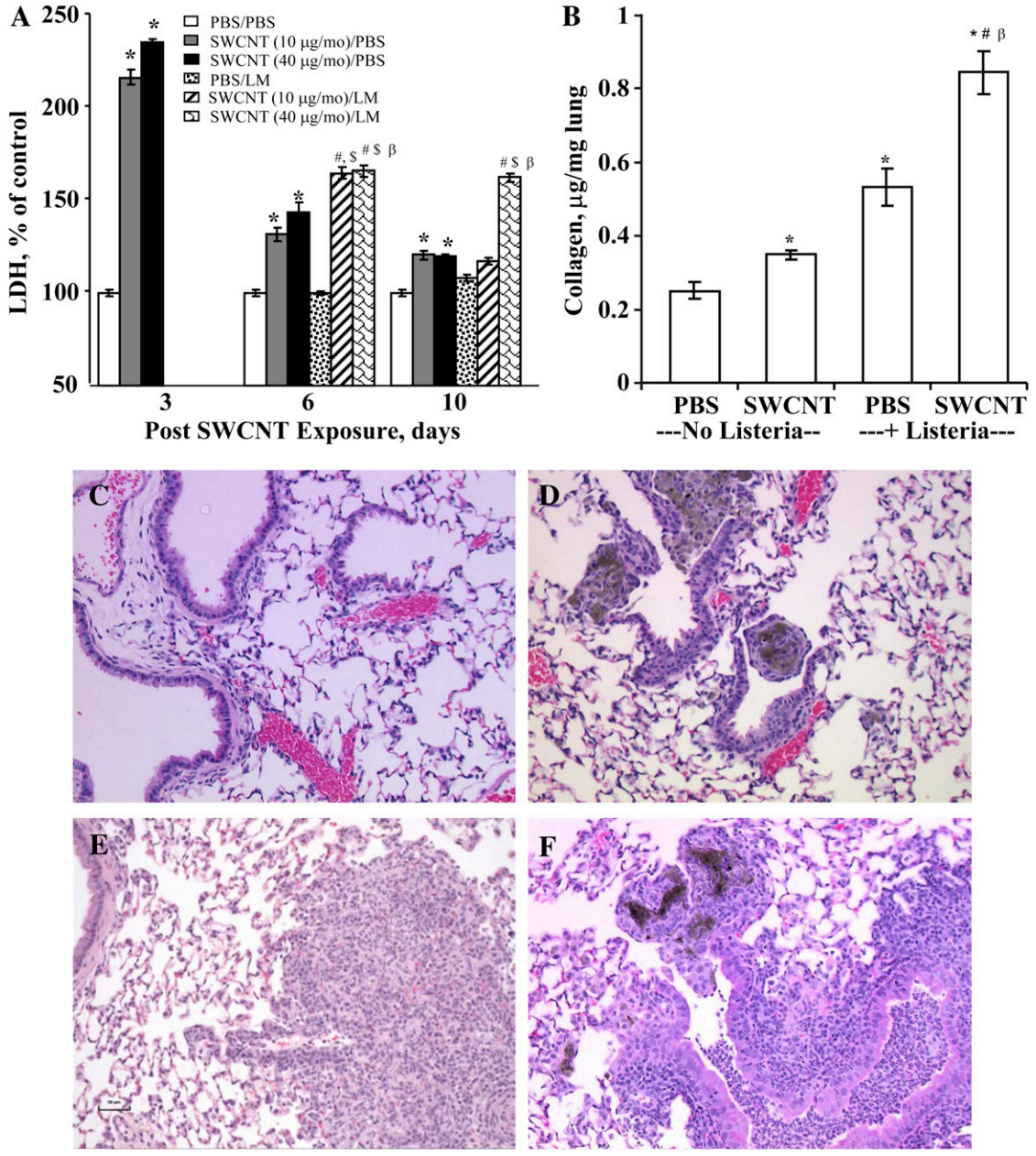

Figure 2. (*A*) Changes in the level of lactate dehydrogenase activity in the bronchoalveolar lavage (BAL) samples of C57BL/6 mice after pharyngeal aspiration with SWCNT and/or LM. *Open bars* represent uninfected animals pre-treated with PBS (PBS/PBS group); *gray bars* represent uninfected animals that had received a low dose of SWCNT (SWCNT, 10 μg/mouse/PBS group); *solid bars* represent uninfected animals that had received a high dose of SWCNT (SWCNT, 40 μg/mouse/PBS group); *dotted bars* represent infected animals pre-treated with PBS (PBS/LM group); *diagonal bars* represent infected animals that had received a low dose of SWCNT (SWCNT, 10 μg/mouse/LM group); *brick bars* represent infected animals that had received a high dose of SWCNT (SWCNT, 40 μg/mouse/LM group). (*B*) Level of collagen in the lung of mice after pharyngeal aspiration with SWCNT (40 μg/mouse) and/or LM (10 d after SWCNT exposure). Data represent mean ± SEM obtained from six mice per group. $^{*}P < 0.05$ versus PBS/PBS control group; $^{\#}P < 0.05$ versus PBS/LM-treated animals; $^{\$}P < 0.05$ versus SWCNT, 10 μg/mouse/PBS-treated mice; $^{\beta}P < 0.05$ versus SWCNT, 40 μg/mouse/PBS-treated mice. (*C–F*) Light micrographs of lung of C57BL/6 mice after pharyngeal aspiration with high dose (40 μg/mouse) of SWCNT and/or LM stained with hematoxylin and eosin at Day 10 of the experiment: *C*, PBS/PBS group; *D*, SWCNT/PBS group; *E*, PBS/LM group; *F*, SWCNT/LM group. *Original magnification*: ×200.

groups treated with LM, edema, inflammation with significant infiltration of PMNs, and multiple granulomatous lesions were observed (Figure 2F). The lesions that were observed in the infected mice pre-treated with SWCNT were more extensive and more pronounced than those observed in the LM alone group, as was assessed by PMNs influx (16.4 ± 1.5% increase).

Collagen deposition. Collagen deposition and pulmonary fibrosis are typical features of inflammatory response to various injuries to the lung, including infections and particles (20). The resolution of a fibroproliferative response after lung injury is key to survival. Exposure to either SWCNT or LM alone significantly increased collagen deposition on Day 10 of the experiment (Figure 2B). Importantly, co-exposure to SWCNT (40 μg/mouse) and LM further increased collagen deposition, reflecting a much stronger profibrotic response.

Cytokines. Cytokines and chemokines are major mediators of the host defense response to microbial pathogens, as well as the tissue reactions following environmental insult. Multiplexing technology was used for simultaneous measurement of 23 cytokines to compare lung BAL cytokine profiles from uninfected or infected mice pre-treated with SWCNT or PBS. The graph in Figure 3 presents the BAL cytokine expression profiles from uninfected animals 3 days after exposure to saline or SWCNT (40 μg/mouse). Of the 23 cytokines measured, basal control levels for most, with the exception of IL-12p40, were either undetectable or relatively low. Significant elevations were noted in several mediators upon exposure to SWCNT alone. The most significant inductions were observed for granulocyte colony-stimulating factor (G-CSF), monocyte chemotactic protein (MCP)-1, macrophage inflammatory protein (MIP)-1α, kera-

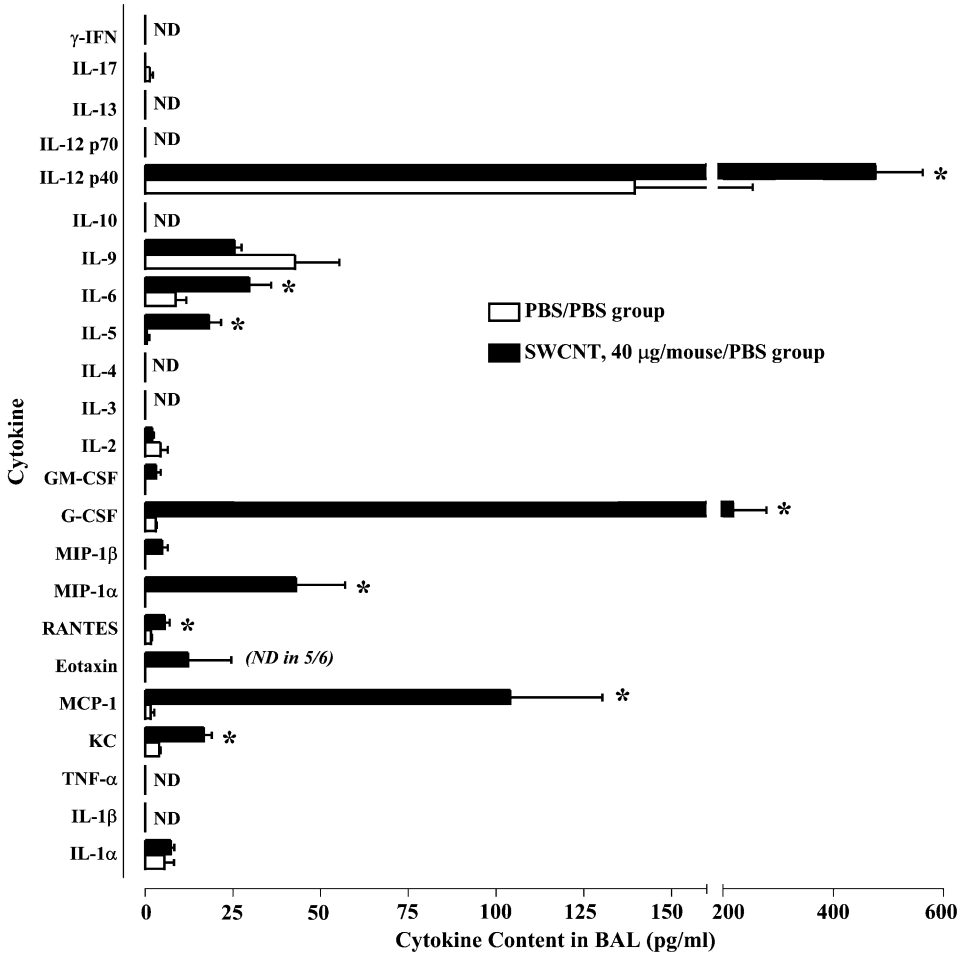

Figure 3. Cytokine profile in BAL of non-infected C57BL/6 mice 3 days after pharyngeal aspiration with SWCNT (40 μg/mouse, *solid bars*) or PBS (*open bars*). IFN-γ, IL-13, IL-12p70, IL-10, IL-4, IL-3, TNF-α, and IL-1β were not detected. ND = below the limit of detection. Data represent mean ± SEM obtained from six animals in the SWCNT-treated group and three in the untreated control group. *$P < 0.05$ versus PBS/PBS group, as determined by unpaired Student's *t* test with Welch's correction for unequal variances between the two groups.

tinocyte chemoattractant (KC), IL-5, and IL-6. While SWCNT increased IL-12p40 approximately 3.5-fold, the level of IL-12p70 was not detectable.

Infected animals pre-exposed to saline or SWCNT differentially induced 13/23 cytokines relative to uninfected mice pre-treated with saline. These could be broadly grouped into three functional categories corresponding to their putative roles in host defense and inflammation, including chemotactic factors (CXCL1, CCL2, CCL3, CCL4, CCL5 [also known as KC, MCP-1, MIP-1α, MIP-1β, and RANTES, respectively]), acute phase reactants (IL-1α, IL-1β, IL-6, and G-CSF), and immune modulators (IL-12 p40 and p70 subunits, IL-17, and IFN-γ).

Figure 4 shows the time course of 2 chemotactic factors, MIP-1α and MCP-1, as well as the p40 and p70 forms of IL-12 in BAL 3, 5, and 7 days after infection with LM (Experimental Days 6, 8, and 10). The responses of the remaining nine cytokines are shown in Table 1. Most of the chemotatic factors and acute phase reactants were elevated at the earliest time point after infection compared with uninfected animals pre-treated with PBS (PBS/PBS group). The effects of SWCNT alone were negligible over these times, since most cytokines were undetectable or equivalent to those seen in PBS/PBS. LM infection produced a robust induction of several cytokines, including MIP-1α (Figure 4A) and MCP-1 (Figure 4B), among others (Table 1), at the early 3-day time point after infection, and there were little or no differences between SWCNT exposure groups for LM induction. During the 7 days (Experimental Day 10) after LM infection alone or with 10 μg/mouse SWCNT pre-exposure, most factors fell to levels approximating those seen in uninfected animals pre-treated with PBS. In contrast, expression of most mediators were greatly elevated after 7 days of infection with LM (Experimental Day 10) in infected mice pre-treated with 40 μg/mouse of SWCNT relative to both uninfected and infected mice pre-treated with PBS. The exception was the level of CCL2 (Figure 4B), which fell throughout the time course of infection, but was still significantly higher in infected animals pre-exposed to high dose SWCNT.

The responses of the immune-modulating cytokines to co-exposures were mixed (Figures 4C and 4D, and Table 1). Mature IL-12 is a heterodimeric protein composed of two subunits termed p40 and p35. LM infection alone induced the IL-12p40 subunit-containing proteins (Figure 4C) and the mature IL-12p70 (Figure 4D) by Day 3 after inoculation (Day 6 of the experiment). It should be noted that the amount of IL-12p40 is almost 50-fold greater than that represented by mature IL-12p70. The levels of both proteins fell toward baseline over the next 4 days. Pre-exposure to SWCNT in uninfected animals did not affect IL-12p40 or IL-12p70 at these times. In contrast, co-exposure to LM and 40 μg/mouse of SWCNT caused a second wave of IL-12p40, but not IL-12p70 expression at 7 days after LM inoculation (Experimental Day 10). Induction of IL-17 (Table 1) was unique in that co-exposure caused a progressive increase from Day 3 to Day 5 (Days 6 and 8 of the experiment, respectively) and then an apparent plateau of expression. IFN-γ expression (Table 1) was also unique, with no effect of either agent alone or low dose co-exposure, but a progressive increased expression in response to the high dose of SWCNT in infected mice.

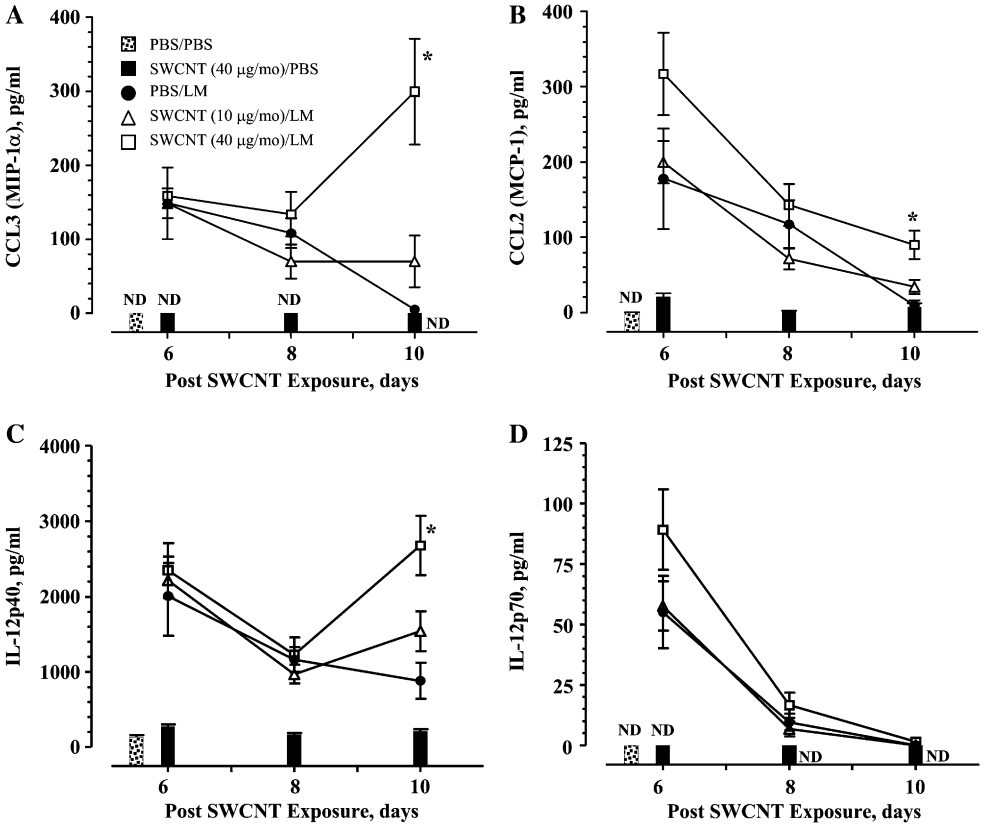

Figure 4. Effect of SWCNT pre-exposure on temporal pattern of four representative cytokines in BAL during LM infection. *A*, CCL-2 (MIP-1α); *B*, CCL-2 (MCP-2); *C*, IL-12 p40; *D*, IL-12 p70. *Dotted bar* represents uninfected animals pre-treated with PBS (PBS/PBS group). *Solid bars* represent uninfected animals that had received high dose of SWCNT (SWCNT, 40 μg/mouse/PBS). *Solid circles* represent infected animals pre-treated with PBS vehicle 3 days before LM administration (PBS/LM group). *Open triangles* represent infected animals that had received a low dose of SWCNT 3 days before infection (SWCNT, 10 μg/mouse/LM group). *Open squares* represent infected animals that had received a high dose of SWCNT before infection (SWCNT, 40 μg/mouse/LM group). Data represent mean ± SEM obtained from six animals in each group. *$P < 0.05$ versus LM/PBS group as assessed by one-way ANOVA and Dunnett's multiple comparisons to the LM alone group.

BAL Cellular Oxidant Production in Response to SWCNT and LM Exposure

We further used CL assay to evaluate ROS production and oxidative burst elicited by BAL cells from animals exposed to SWCNT and/or LM. We found that the CL was increased 6.4-fold 3 days after exposure to 40 μg/mouse of SWCNT in uninfected mice and returned to control (PBS) level by Day 6 (Figure 5A). LM exposure alone also increased BAL cell chemiluminesence by 3.2-fold at 3 days after infection (Day 6 of experiment). However, this LM-induced ROS generation was not altered by pre-exposure to SWCNT.

Effects of SWCNT on Pulmonary Clearance of LM

Bacterial CFU were measured in the lung homogenates to determine whether SWCNT exposure affected functional LM infection rates. No differences in infectivity were observed 3 days after LM infection (corresponds to 6 d of experiment) in the mice pre-treated with PBS or low dose of SWCNT (10 μg/mouse). However, the bacterial load in the lungs of mice pre-exposed to 40 μg/mouse of SWCNT was significantly elevated 3 and 7 days after infection (Days 6 and 10 of the experiment), demonstrating a SWCNT-dependent suppression of bacterial clearance (Figure 5B).

The Ability of Macrophages to Phagocytize LM

The ability of macrophages from SWCNT-exposed animals to phagocytize LM was compared with that of control animals. Cell Tracker Green was used to visualize cellular uptake of LM. As shown in Figure 6A, uptake of LM by macrophages was readily detectable by co-localization of red and green fluorescence, yielding yellow fluorescence. A summary of these measurements is shown on Figure 6B, which demonstrates that AMs from SWCNT-exposed animals were less effective in phagocytosis than macrophages from control (PBS-treated) mice. Similar results were obtained in experiments in which we isolated AMs from naïve mice and then compared their phagocytizing activity toward LM with and without pre-exposure to SWCNT (0, 90, or 240 μg/ml, 1 h). Again, we found that pre-exposure of macrophages to SWCNT *in vitro* resulted in a decreased phagocytozing activity (Figure 6B, *inset*).

NO Production by Macrophages

We further assessed production of NO by macrophages using DAF-2-DA (2 μM; EMD Biosciences, San Diego, CA) as a specific intracellular indicator (Figure 6C). Interestingly, production of NO by macrophages in response to LM was also dependent on pre-exposure to SWCNT: the level of NO production was lower in macrophages obtained from SWCNT-exposed mice than in control (PBS-treated) animals. *In vitro* pre-incubation of alveolar macrophages with SWCNT also caused decreased production of NO in response to LM, as evidenced by decreased fluorescence of adducts formed with DAF-2 (Figure 6C, *inset*).

DISCUSSION

As an understanding of the potential health risks associated with the fabrication and use of engineered nanomaterials, including SWCNT, emerges, there is an increasing need for their detailed toxicological assessment. Realistic exposures to SWCNT are likely to occur in conjunction with other pathogenic impacts, such as microbial infections. Since both SWCNT and infections induce inflammatory response and oxidative stress, their interactions may trigger interactive reactions that are difficult to assess by simple additive extrapolations. Here, we report that sequential exposure to SWCNT and LM triggered an enhanced inflammatory response. The amounts of inflammatory cells in BAL, collagen deposition,

TABLE 1. EFFECT OF SWCNT PRE-EXPOSURE ON BAL LEVEL OF SELECT CYTOKINES (PG/ML) DURING LM INFECTION

Cytokine	Treatment	Day 6	Day 8	Day 10
CCL4	PBS/PBS	ND		
(MIP-1β)	PBS/LM	9 ± 3	11 ± 3	1 ± 1
	LM /SWCNT (low)	8 ± 1	9 ± 3	4 ± 1
	LM /SWCNT (high)	8 ± 1	13 ± 3	18 ± 5*
	SWCNT (high)/PBS	ND	ND	ND
CCL5	PBS/PBS	2 ± 1		
(RANTES)	PBS/LM	26 ± 7	34 ± 4	13 ± 4
	LM /SWCNT (low)	31 ± 4	27 ± 5	43 ± 11
	LM /SWCNT (high)	32 ± 3	45 ± 9	81 ± 10*
	SWCNT (high)/PBS	4 ± 1	ND	3 ± 2
CXCL-1	PBS/PBS	5 ± 1		
(KC)	PBS/LM	56 ± 16	54 ± 8	19 ± 7
	LM + SWCNT (low)	46 ± 7	37 ± 8	27 ± 9
	LM + SWCNT (high)	62 ± 8	55 ± 10	168 ± 44*
	SWCNT (high)/PBS	9 ± 1	16 ± 2	9 ± 2
IL-1α	PBS/PBS	3 ± 1		
	PBS/LM	12 ± 3	10 ± 1	3 ± 1
	LM + SWCNT (low)	10 ± 1	9 ± 2	6 ± 1
	LM + SWCNT (high)	12 ± 1	12 ± 2	16 ± 4*
	SWCNT (high)/PBS	4 ± 1	3 ± 1	2 ± 1
IL-1β	PBS/PBS	2 ± 1	—	
	PBS/LM	9 ± 3	20 ± 4	1 ± 1
	LM + SWCNT (low)	2 ± 2	15 ± 2	2 ± 1
	LM + SWCNT (high)	2 ± 1	10 ± 3	25 ± 9*
	SWCNT (high)/PBS	ND	ND	ND
IL-6	PBS/PBS	7 ± 2	—	
	PBS/LM	372 ± 154	391 ± 70	14 ± 6
	LM + SWCNT (low)	248 ± 22	327 ± 68	59 ± 35
	LM + SWCNT (high)	401 ± 82	627 ± 119	379 ± 119*
	SWCNT (high)/PBS	8 ± 1	4 ± 1	8 ± 2
G-CSF	PBS/PBS	2 ± 1		
	PBS/LM	722 ± 318	301 ± 36	68 ± 29
	LM + SWCNT (low)	451 ± 72	223 ± 47	194 ± 92
	LM + SWCNT (high)	618 ± 89	407 ± 97	754 ± 234*
	SWCNT (high)/PBS	6 ± 1	4 ± 1	4 ± 1
IL-17	PBS/PBS	ND		
	PBS/LM	12 ± 4	44 ± 16	6 ± 2
	LM + SWCNT (low)	18 ± 4	34 ± 6	18 ± 8
	LM + SWCNT (high)	24 ± 3	66 ± 20	54 ± 15*
	SWCNT (high)/PBS	ND	ND	ND
IFN-γ	PBS/PBS	ND		
	PBSLM	15 ± 6	15 ± 5	3 ± 1
	LM + SWCNT (low)	13 ± 6	15 ± 5	5 ± 2
	LM + SWCNT (high)	51 ± 21	148 ± 71	676 ± 407*
	SWCNT (high)/PBS	ND	ND	ND

Data represent mean ± SEM ($n = 9$ for PBS/PBS group, $n = 4$–5 for SWCNT/PBS group, and $n = 6$ for all other groups). Low and high SWCNT dose correspond to 10 and 40 μg/mouse, respectively. ND, below the lower limit of detection.

* $P < 0.05$ versus PBS/LM group from that same time.

and cytokine responses were all markedly enhanced compared with the respective responses to each of the components alone.

We previously demonstrated that toxic responses to SWCNT could be modulated by a number of factors such as genetic and nutritional status (21) (e.g., vitamin E levels, expression of NADPH oxidase). Thus, individual susceptibility to toxic effects of SWCNT may vary. Here, we documented that bacterial infection can act as an additional important factor to enhance inflammatory response to SWCNT adding yet another aspect of modified sensitivity to SWCNT toxicity. Different modes of exposure to SWCNT and LM—simultaneous or sequential—may result in different patterns of deposition and clearance. In this study, we were mostly interested in the interaction between SWCNT-induced inflammatory response and infectivity. Therefore, we chose the regimen of pre-exposure to SWCNT associated with pronounced inflammatory and oxidative stress responses. Moreover, our previous studies (13) have demonstrated that after 3 days of exposure to SWCNT, a significant part of nanotubes in the lung is sequestered in granulomas thus limiting direct physical contact and potential adsorption of LM on SWCNT.

The importance of enhanced responses to a sequential exposure to SWCNT and LM dictates the necessity to better understand the pathways involved in their interactions. Recently, attempts have been made to use nanoparticles for targeted drug delivery to specific cells of the immune system. Macrophages may be very promising targets for drug-loaded nanoparticles due to their central role in inflammation and their ability to harbor a variety of bacteria, viruses, and parasites. This sequestering of infectious agents is significant for risk of contracting a number of deadly diseases in humans, such as leishmaniasis, tuberculosis, and HIV (22, 23). Special consideration, however, should be given to the inflammatory potential of drug-laden nanoparticles with SWCNT-like properties, since SWCNT may modulate the sensitivity of the body's immune responses to infections. The current findings indicate that SWCNT exacerbate pro-inflammatory and pro-oxidant injuries or effects. In addition, synergies in induction and release of specific cytokines may be an important participating mechanism underlying the risks of unexpected side effects of co-exposures of the SWCNT-like nanoparticles with bacteria or other environmental insults.

While engineered nonmodified SWCNT used in the study may compromise innate immune response and clearance of bacterial pathogens, thus raising questions regarding possible health aspects for producers and users (24), there are many examples of successful use of nanomaterials for delivery of anti-inflammatory agents such as antibiotics as well as steroidal (25) and nonsteroidal anti-inflammatory drugs (NSAIDs) (26). In addition, immunonanoparticles (i.e., nanoparticles functionalized with pathogen-specific antibodies) may serve as antimicrobial carriers for improving the stability and activity of antimicrobials in foods. A recent study documented that the use of polystyrene immunonanoparticles with active carboxyl groups conjugated with anti-LM antibody and coated with lysozyme was more effective than direct addition of lysozyme for inactivating *L. monocytogenes* (27). Moreover, some nanoparticles (e.g., cerium oxide [CeO_2]) exert significant anti-inflammatory and antioxidant properties (28). Further, different types of nanoparticles (e.g., silver nanoparticles, W(4+)-doped titanium-coated nickel ferrite composite nanoparticles) without any specific loads reportedly exert antimicrobial activity by themselves or in combination with photo-therapy (29–32). Finally, antimicrobial effects of nanoparticles seem to be dependent on the type of bacterial pathogen. A recent report, documented that pristine SWCNT can exhibit strong antimicrobial activity toward *Escherichia coli* (33). The authors speculate that direct cell contact with SWCNT can cause severe membrane damage and subsequent cell inactivation. Obviously, further research on interactions of different types of nonmodified, purposely modified nanoparticles and nanoparticles loaded with bioactive cargoes with different bacterial pathogens is warranted.

The mechanism by which pre-exposure to SWCNT decreases subsequent bacterial clearance is unclear. Our experiments demonstrate that impaired innate clearance of LM in mice pre-exposed to SWCNT may be due, at least in part, to a decreased potency of macrophages in handling this bacterial pathogen. This was evidenced by a decreased capacity of alveolar macrophages obtained from mice pre-treated with SWCNT to phagocytize LM. Interestingly, even pre-incubation of "normal" AMs isolated from naïve mice to SWCNT affected their phagocytozing function and decreased uptake of LM. Specific mechanisms underlying the effects of SWCNT on macrophage functions remain to be elucidated. Interestingly, no effects of SWCNT on superoxide production by AMs were detected (data not shown).

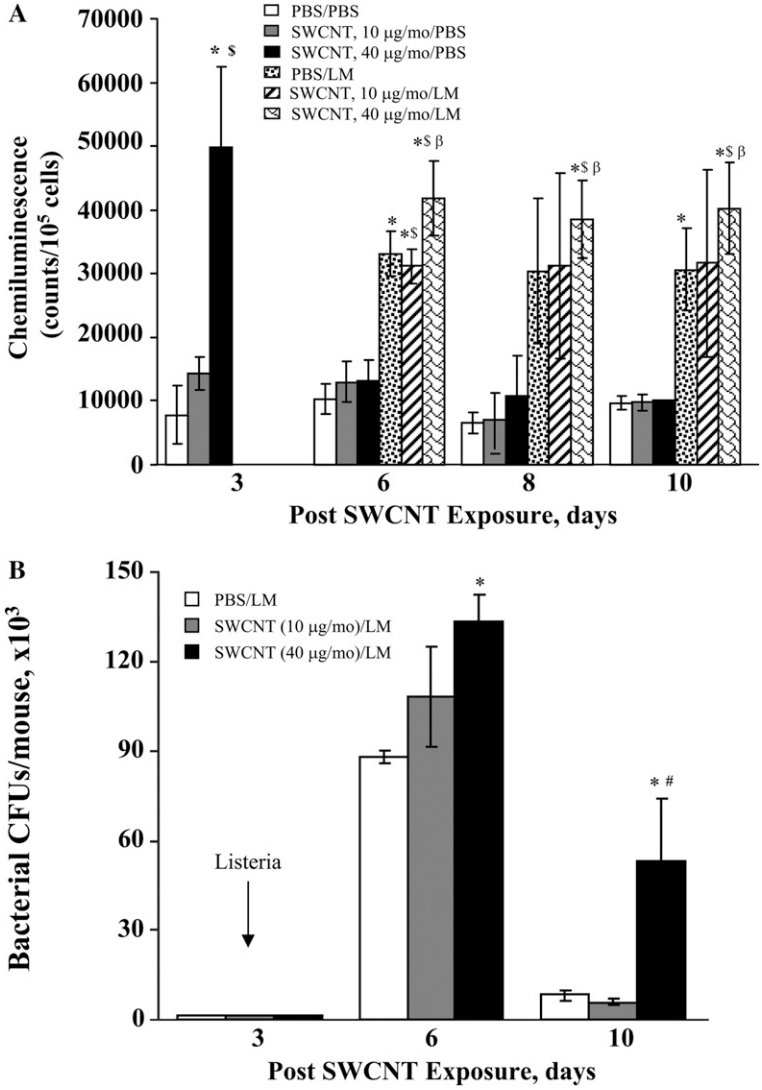

Figure 5. (*A*) Reactive oxygen species production in the BAL cells in response to SWCNT and/or LM exposure. *Open bars* represent uninfected animals pre-treated with PBS (PBS/PBS group); *gray bars* represent uninfected animals that had received a low dose of SWCNT (SWCNT, 10 μg/mouse/PBS group); *solid bars* represent uninfected animals that had received a high dose of SWCNT (SWCNT, 40 μg/mouse/PBS group); *dotted bars* represent infected animals pre-treated with PBS (PBS/LM group); *diagonal bars* represent infected animals that had received a low dose of SWCNT (SWCNT, 10 μg/mouse/LM group); *brick bars* represent infected animals that had received a high dose of SWCNT (SWCNT, 40 μg/mouse/LM group). $^{*}P < 0.05$ versus PBS/PBS control group; $^{\$}P < 0.05$ versus SWCNT, 10 μg/mouse/PBS-treated mice; $^{\beta}P < 0.05$ versus SWCNT, 40 μg/mouse/PBS-treated mice. (*B*) Assessment of pulmonary bacterial clearance in lung of C57BL/6 mice after challenge with SWCNT. *Open bars* represent infected animals pre-treated with PBS (PBS/LM group); *gray bars* represent infected animals that had received a low dose of SWCNT (SWCNT, 10 μg/mouse/LM group); *solid bars* represent infected animals that had received a high dose of SWCNT (SWCNT, 40 μg/mouse/LM group). $^{*}P < 0.05$ versus PBS/LM group; $^{\#}P < 0.05$ versus SWCNT, 10 μg/mouse/LM-treated animals.

The ability of alveolar macrophages to generate NO, however, was significantly compromised after SWCNT pre-exposures of mice *in vivo* or pre-incubation with macrophages *in vitro*. This suggests that NO-dependent (rather than superoxide-dependent) pathways affected by SWCNT in macrophages might be involved in decreased clearance of LM in SWCNT pre-exposed mice.

It is possible that killing of LM depends more on production of nitric oxide (NO) than ROS from the oxidative burst, since genetic deletion of iNOS produces a more severe decrement in resistance to LM than deficiency of p47phox, a major component of the 47-kD phagocyte NADPH oxidase (34, 35). On the other hand, Saxena and coworkers showed that exposure of mouse AMs to diesel exhaust particles attenuated IFN-γ–induced production of NO (36). In addition, pulmonary exposure of rats to diesel exhaust particles depressed NO production by AMs in response to pulmonary LM infection and depressed bacterial clearance (37). Similarly, pulmonary exposure to ROFA enhanced zymosan-stimulated chemiluminescence in rat AMs but reduced NO release and bacterial clearance in response to the same stimulus (38).

Host resistance to the intracellular bacterium, LM, involves both innate and adaptive immune mechanisms (39). This organism has been used to demonstrate the ability of other particulate toxins such as diesel exhaust particles (37), residual oil fly ash (38), and welding fumes (40) to inhibit host defense mechanisms and increase the severity of pulmonary infections. Initial innate immune responses to infection include accumulation and activation of neutrophils, natural killer (NK) cells, and macrophages to sites of infection with attendant up-regulation of bacteriocidal activities. If organism load is large or infection persists, then secondary Th1-type dominant adaptive immune strategies are required for protection. Evidence for this secondary response includes a requirement for induced TNF-α (41) and IFN-γ (42) expression to mediate resistance to LM.

Our data demonstrate that pre-exposure to SWCNT greatly attenuated the clearance of LM from the lung. Using larger doses of LM in a rat model, Yin and colleagues attributed the immunosuppressive effects of acute exposure to diesel exhaust particles to attenuation of early macrophage activation and cytokine release (43). The cytokine profiles obtained in our study 3 days after infection (Experimental Day 6) appeared to be very similar between uninfected animals pre-treated with PBS or both doses of SWCNT. We could not readily detect TNF-α or IL-1β at the early 3-day time point of experiment, but robust elevations in IL-6, G-CSF, MCP-1, and other chemokines were observed in all cases. This cytokine profile might reflect a less robust Th1 response arising from SWCNT treatment. However, this decrease was similar with both doses of SWCNT, whereas only high-dose SWCNT showed significant compromise of host defense. In

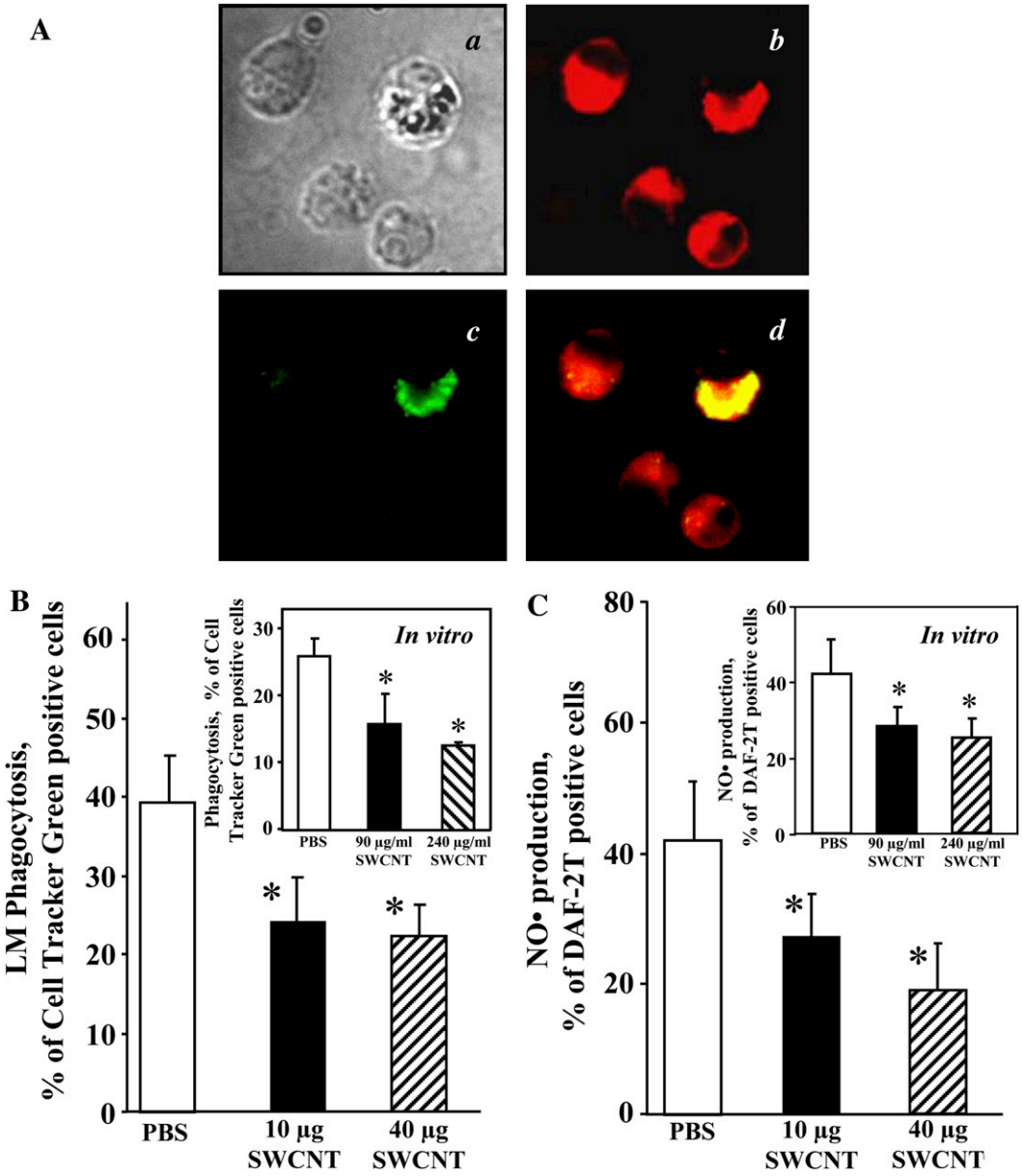

Figure 6. Effect of SWCNT on phagocytosis of LM and production of NO· by alveolar macrophages from mouse BAL. (*A*) Typical fluorescence micrographs of alveolar macrophages pre-treated with SWCNT and co-incubated with LM: *a*, bright field image; *b*, red fluorescence image (Nile Red staining of macrophages); *c*, green fluorescence image (Cell Tracker Green labeled LM); *d*, overlay of red and green images. (*B*) Phagocytosis of LM by alveolar macrophages obtained from C57BL/6 mice pre-exposed to SWCNT *in vivo*. Three hundred macrophages per sample were counted. Data are mean ± SD, $n = 3$. *$P < 0.05$ versus control PBS/LM-treated group. *Inset:* Phagocytosis of LM by alveolar macrophages exposed to SWCNT *in vitro*. Three hundred macrophages per sample were counted. Data are mean ± SD, $n = 3$. (*C*) NO· production by alveolar macrophages obtained from C57BL/6 mice pre-exposed to SWCNT *in vivo*. Three hundred macrophages per sample were counted. Data are mean ± SD, $n = 3$. *$P < 0.05$ versus control PBS/LM-treated group. *Inset:* NO· production by alveolar macrophages exposed to SWCNT *in vitro*. Three hundred macrophages per sample were counted. Data are mean ± SD, $n = 3$.

addition, IL-12p40 subunit was equivalently induced in all groups. Thus, it appears that the overall ability of LM to initiate early cytokine responses after infection is not greatly affected by SWCNT exposure. This suggests that the initial innate signaling mechanisms for pathogen recognition and responses remain intact. In contrast, it is possible that target cell responses to these cytokines are decreased by SWCNT.

The failure to clear LM early after infection in mice pre-exposed to SWCNT leads to a continued elevation in nearly all the chemokines and acute phase cytokines into the later course of infection. In fact many of these, such as KC, CCL3, CCL4, and CCL5, are significantly higher in the high-dose SWCNT mice on Day 7 after infection (Experimental Day 10) compared with the levels seen in the same group 3 days after infection (Experimental Day 6), despite the fact that organism load appears similar. A significant induction of a number of cytokines/chemokines on Experimental Day 6 coincided with the increase in cell recruitment at this time point, which, however, was not different for ± SWCNT experimental groups. Importantly, assessments of the cells already present in the lung probably reflect cytokine/chemokine production at some point earlier. It is possible that differential cytokine production occurred earlier, for example on Days 3 to 5. For example, it is clear that the exposure to SWCNT alone for 3 days was accompanied by a robust induction of chemokines and other inflammatory mediators (Figure 3). Thus, it is likely that SWCNT-dependent influx of some inflammatory cells had already occurred in the lung at the time of LM infection. The reasons for the synergistic effects on cytokine release are unclear, but could reflect the shift from innate immune mechanisms to adaptive Th1 lymphocyte–dominant immune-dependent responses. The accumulation of lymphocytes antecedes the accumulation of other inflammatory cells, and was most obvious in the SWCNT-treated groups at the latest time point. Moreover, the levels of IL-17 and IFN-γ in BAL paralleled this pattern and were significantly elevated after high-dose SWCNT compared with LM-infected animals pre-treated with PBS. Both of these lymphokines are known to potentiate release of inflammatory mediators from target cells on combination with other inducing stimuli (44, 45). We observed an early induction of IL-12p70, a primary determinant of Th1-biased response, in all the LM-

infected groups. Only mice pre-exposed to high-dose SWCNT, however, showed a sequential release of the Th1 effector product, IFN-γ. Therefore, IL-12p70 alone is not sufficient for the maximal appearance of IFN-γ. In addition, other sources of IFN-γ, such as NK and γδ-T cells, also need to be considered as potential sources of IFN-γ during mixed exposures to LM and SWCNT. Our data also indicate that the newly described Th17-dependent immune response (46) is activated during LM infection in the lung, especially during SWCNT exposure.

Previous work from our group has established that SWCNT exposure promotes tissue fibrosis and granuloma formation associated with the release of high levels of TGF-β (19). While TGF-β is well known for its ability to direct tissue remodeling and repair, it also possesses immunoregulatory properties. TGF-β produced by regulatory T cells (Tregs) has immunosuppressant properties by suppressing Th1 effector cell responses (47) and could, thus, limit adaptive immune responses to LM in the SWCNT-exposed lung. Moreover, in the presence of IL-6, it functions to drive Th17 differentiation (48) and may account for the elevated levels of IL-17 observed in infected animals exposed to a high dose of SWCNT. Thus, it is possible that SWCNT-dependent chronic inflammation/fibrosis can modulate the magnitude and type of adaptive immune responses generated upon challenge of that organ to a microbial pathogen. While not specifically measured in this study, we have shown that TGF-β peaks 3 days after SWCNT exposure (i.e., the same time as when we inoculated the lungs with LM) (13). It is also evident that the lung environment produced by SWCNT alone contained high levels of other immunomodulatory mediators, such as IL-12 family members, G-CSF, IL-6, IL-5, MIP-1α, and MCP-1, at the time of LM infection (i.e., Day 3 of experiment) (Figure 3), that may also modulate the repertoire of host-defense responses to microbial pathogens.

Th2 immune responses and IL12-p40 are associated with fibrotic tissue remodeling (49, 50), while Th1 responses are a requisite for efficient clearance of facultative intracellular pathogens like *Listeria*. We can speculate that the Th2/Th1 bias of immune response is altered during SWCNT/LM co-exposure. The burst of IFN-γ in co-exposed animals may reflect aspects of Th1-based immunity; however, the SWCNT-associated component of inflammation may have modified the immune response to favor the development of pro-fibrogenic environment, as illustrated by declining levels of IL-12p70 and augmentation of IL-12p40. In addition, SWCNT exposure alone produced alterations in several cytokines, like IL-5, MCP-1, IL-6, and G-CSF, previously associated with Th2 responses (51–53). The fact the IL-12p40 homodimers can antagonize the biologic effects of IL-12p70 may also be of relevance here (54), since we frequently observed induction of IL-12p40 in absence of any changes in mature IL-12p70.

In line with this, we found a markedly increased level of collagen deposition in the lung of mice exposed to SWCNT/LM. These results were confirmed by morphometric assessments of alveolar wall thickening (data not shown). While the collagen measurements were performed on Day 10 of the experiment, which may be viewed as an early time point to characterize fibrotic development in the lung, our previous studies have established that the early SWCNT-induced collagen deposition did not resolve and progressed over at least 60 days (13). Thus it is likely that LM enhances SWCNT-induced early fibrotic response.

SWCNT doses used in the study are occupationally (rather than environmentally) relevant. Previously we have reported that a 20-μg dose of SWCNT given by pharyngeal aspiration route to C57BL/6 mice deposited in the alveolar region, corresponding to approximately the same estimated dose for a worker exposed to the OSHA PEL for graphite (5 mg/m^3, 8 h workday, 40 h per week) over a period of 20 work days (13). According to our earlier published data on the airborne SWCNT concentrations in a laboratory producing SWCNT, peak airborne concentrations of 53 mg/m^3 were measured. Aspirated doses of 10 and 40 μg SWCNT/mouse are relevant to predicted deposited doses after 2 and 8 years of exposure at peak airborne concentrations measured in these occupational settings (55).

In summary, our findings clearly demonstrate that sequential exposure to SWCNT and LM induced unusual responses in which both components—nanoparticles and bacterial infection—mutually enhanced inflammation and depress bacterial clearance.

Conflict of Interest Statement: None of the authors has a financial relationship with a commercial entity that has an interest in the subject of this manuscript.

References

1. Maynard AD. Nanotechnology: the next big thing, or much ado about nothing? *Ann Occup Hyg* 2007;51:1–12.
2. Donaldson K, Aitken R, Tran L, Stone V, Duffin R, Forrest G, Alexander A. Carbon nanotubes: a review of their properties in relation to pulmonary toxicology and workplace safety. *Toxicol Sci* 2006;92:5–22.
3. Lam CW, James JT, McCluskey R, Arepalli S, Hunter RL. A review of carbon nanotube toxicity and assessment of potential occupational and environmental health risks. *Crit Rev Toxicol* 2006;36:189–217.
4. Kagan VE, Tyurina YY, Tyurin VA, Konduru NV, Potapovich AI, Osipov AN, Kisin ER, Schwegler-Berry D, Mercer R, Castranova V, *et al.* Direct and indirect effects of single walled carbon nanotubes on RAW 264.7 macrophages: role of iron. *Toxicol Lett* 2006;165:88–100.
5. Walsh TJ, Viviani MA, Arathoon E, Chiou C, Ghannoum M, Groll AH, Odds FC. New targets and delivery systems for antifungal therapy. *Med Mycol* 2000;38:335–347.
6. McCarron PA, Donnelly RF, Canning PE, McGovern JG, Jones DS. Bioadhesive, non-drug-loaded nanoparticles as modulators of candidal adherence to buccal epithelial cells: a potentially novel prophylaxis for candidosis. *Biomaterials* 2004;25:2399–2407.
7. Scott CD, Povitsky A, Dateo C, Gokcen T, Willis PA, Smalley RE. Iron catalyst chemistry in modeling a high-pressure carbon monoxide nanotube reactor. *J Nanosci Nanotechnol* 2003;3:63–73.
8. Gorelik O, Nikolaev P, Arepalli S. Purification procedures for single-walled carbon nanotubes. NASA contractor report; 2000. NASA/CR-2000–208926.
9. Birch ME. Elemental carbon: monitoring of diesel exhaust particulate in the workplace. In: NIOSH manual of analytical methods (NMAM 5040), 4th ed. Cincinnati, OH: NIOSH; 2003. pp. 1–5. DHHS publication No 2003–154.
10. Arepalli S, Nikolaev P, Gorelik O. Protocol for the characterization of SWCNT material quality. *Carbon* 2004;42:1783–1791.
11. Arepalli S, Nikolaev P, Gorelik O. Analytical characterization of single wall carbon nanotubes. *Encyclopedia of Nanosci and Nanotechnol* 2004;1:51–66.
12. Rao GV, Tinkle S, Weissman DN, Antonini JM, Kashon ML, Salmen R, Battelli LA, Willard PA, Hoover MD, Hubbs AF. Efficacy of a technique for exposing the mouse lung to particles aspirated from the pharynx. *J Toxicol Environ Health* 2003;66:1441–1452.
13. Shvedova AA, Kisin ER, Mercer R, Murray AR, Johnson VJ, Potapovich AI, Tyurina YY, Gorelik O, Arepalli S, Schwegler-Berry D, *et al.* Unusual inflammatory and fibrogenic pulmonary responses to single walled carbon nanotubes in mice. *Am J Physiol Lung Cell Mol Physiol* 2005;289:698–708.
14. Mercer RR, Russell ML, Crapo JD. Alveolar septal structure in different species. *J Appl Physiol* 1994;77:1060–1066.
15. Small JV. Measurements of section thickness. In: Bocciarelli DS, editor. Proceedings of the 4th European Congress on Electron Microscopy. Rome: Tipografia Poliglotta Vaticana; 1968. pp. 609–610.
16. Antonini JM, Van Dyke K, Ye Z, DiMatteo M, Reasor MJ. Introduction of luminal-dependent chemiluminescence as a method to study silica inflammation in the tissue and phagocytic cells of rat lung. *Environ Health Perspect* 1994;102:37–42.
17. Szondy Z, Sarang Z, Molnar P, Nemeth T, Piacentini M, Mastroberardino PG, Falasca L, Aeschlimann D, Kovacs J, Kiss I, *et al.* Transglutaminase $2^{-/-}$ mice reveal a phagocytosis-associated crosstalk

between macrophages and apoptotic cells. *Proc Natl Acad Sci USA* 2003;100:7812–7817.
18. Jourd'heuil D. Increased nitric oxide-dependent nitrosylation of 4,5-diaminofluorescein by oxidants: implications for the measurement of intracellular nitric oxide. *Free Radic Biol Med* 2002;33:676–684.
19. Kojima H, Nakatsubo N, Kikuchi K, Kawahara S, Kirino Y, Nagoshi H, Hirata Y, Nagano T. Detection and imaging of nitric oxide with novel fluorescent indicators: diaminofluoresceins. *Anal Chem* 1998;70:2446–2453.
20. Fries KM, Blieden T, Looney RJ, Sempowski GD, Silvera MR, Willis RA, Phipps RP. Evidence of fibroblast heterogeneity and the role of fibroblast subpopulations in fibrosis. *Clin Immunol Immunopathol* 1994;72:283–292.
21. Shvedova AA, Kisin ER, Murray AR, Gorelik O, Arepalli S, Castranova V, Young SH, Gao F, Tyurina YY, Oury TD, *et al.* Vitamin E deficiency enhances pulmonary inflammatory response and oxidative stress induced by single-walled carbon nanotubes in C57BL/6 mice. *Toxicol Appl Pharmacol* 2007;221:339–348.
22. Chellat F, Merhi Y, Moreau A, Yahia L. Therapeutic potential of nanoparticulate systems for macrophage targeting. *Biomaterials* 2005; 26:7260–7275.
23. Basu MK, Lala S. Macrophage specific drug delivery in experimental leishmaniasis. *Curr Mol Med* 2004;4:681–689.
24. Nasterlack M, Zober A, Oberlinner C. Considerations on occupational medical surveillance in employees handling nanoparticles. *Int Arch Occup Environ Health* 2007;81:721–726.
25. Sashmal S, Mukherjee S, Ray S, Thakur RS, Ghosh LK, Gupta BK. Design and optimization of NSAID loaded nanoparticles. *Pak J Pharm Sci* 2007;20:157–162.
26. Blaschke T, Kankate L, Kramer KD. Structure and dynamics of drug-carrier systems as studied by parelectric spectroscopy. *Adv Drug Deliv Rev* 2007;59:403–410.
27. Yang H, Qu L, Wimbrow A, Jiang X, Sun YP. Enhancing antimicrobial activity of lysozyme against Listeria monocytogenes using immuno-nanoparticles. *J Food Prot* 2007;70:1844–1849.
28. Niu J, Azfer A, Rogers LM, Wang X, Kolattukudy PE. Cardioprotective effects of cerium oxide nanoparticles in a transgenic murine model of cardiomyopathy. *Cardiovasc Res* 2007;73:549–559.
29. Shahverdi AR, Fakhimi A, Shahverdi HR, Minaian S. Synthesis and effect of silver nanoparticles on the antibacterial activity of different antibiotics against Staphylococcus aureus and Escherichia coli. *Nanomedicine* 2007;3:168–171.
30. Sunkara BK, Misra RD. Enhanced antibactericidal function of W(4+)-doped titania-coated nickel ferrite composite nanoparticles: A biomaterial system. *Acta Biomater* 2008;4:273–283.
31. Kim JS, Kuk E, Yu KN, Kim JH, Park SJ, Lee HJ, Kim SH, Park YK, Park YH, Hwang CY, *et al.* Antimicrobial effects of silver nanoparticles. *Nanomedicine* 2007;3:95–101.
32. Lok CN, Ho CM, Chen R, He QY, Yu WY, Sun H, Tam PK, Chiu JF, Che CM. Silver nanoparticles: partial oxidation and antibacterial activities. *J Biol Inorg Chem* 2007;12:527–534.
33. Kang S, Pinault M, Pfefferle LD, Elimelech M. Single-walled carbon nanotubes exhibit strong antimicrobial activity. *Langmuir* 2007;23: 8670–8673.
34. Shiloh MU, MacMicking JD, Nicholson S, Brause JE, Potter S, Marino M, Fang F, Dinauer M, Nathan C. Phenotype of mice and macrophages deficient in both phagocytic oxidase and inducible nitric oxide synthase. *Immunity* 1999;10:29–38.
35. Endres R, Luz A, Schulze H, Neubauer H, Futterer A, Holland SM, Wagner H, Pfeffer K. Listeriosis in p47(phox−/−) and TRp55(−/−) mice: protection despite absence of ROI and susceptibility despite the presence of RNI. *Immunity* 1997;7:419–432.
36. Saxena RK, Saxena QB, Wiessman DN, Simpson JP, Bledsoe TA, Lewis DM. Effect of diesel exhaust particulate on Bacillus Calmette-Guerin lung infection in mice and attendant changes in lung interstitial lymphoid subpopulations and IFNγ response. *Toxicol Sci* 2003;73:66–71.
37. Yang H-M, Antonini JM, Barger MW, Butterworth L, Roberts JR, Ma JKH, Castranova V, Ma JYC. Diesel exhaust particles suppress macrophage function and slow the pulmonary clearance of *Listeria monocytogenes* in rats. *Environ Health Perspect* 2001;109:515–521.
38. Antonini JM, Roberts JR, Jernigan MR, Yang H-M, Ma JYC, Clark RW. Residual oil fly ash increases the susceptibility to infection and severely damages the lungs after pulmonary challenge with a bacterial pathogen. *Toxicol Sci* 2002;70:110–119.
39. Pamer EG. Immune responses to *Listeria monocytogenes. Nat Rev Immunol* 2004;4:812–823.
40. Antonini JM, Taylor MD, Millecchia L, Bebout AR, Roberts JR. Suppression in lung defense responses after bacterial infection in rats pretreated with different welding fumes. *Toxicol Appl Pharmacol* 2004;200:206–218.
41. Pfeffer K, Matsuyama T, Kundiq TM, Wakeham A, Kishihara K, Shainianm A, Wiegmann K, Ohashi PS, Kronke M, Mak TW. Mice deficient for the 55kd tumor necrosis factor receptor are resistant to endotoxic shock, yet succumb to *L. monotocytogenes* infection. *Cell* 1993;73:457–467.
42. Harty JT, Bevan MJ. Specific immunity to *Listeria monocytogenes* in the absence of IFNγ. *Immunity* 1995;3:109–117.
43. Yin X-J, Schafer R, Ma JYC, Antonini JM, Weissman DD, Siegel PD, Barger MW, Roberts JR, Ma JKH. Alteration of pulmonary immunity to *Listeria monocytogenes* by diesel exhaust particles (DEPs). I. Effects of DEPs on early pulmonary responses. *Environ Health Perspect* 2002;110:1105–1111.
44. van den Berg A, Kuiper M, Snoek M, Timens W, Postma DS, Jansen HM, Lutter P. Interleukin-17 induces hyperresponsive interleukin-8 and interleukin-6 production to tumor necrosis factor-alpha in structural lung cells. *Am J Respir Cell Mol Biol* 2005;33:97–104.
45. Schoder K, Sweet MJ, Hume DA. Signal integration between IFNγ and TLR signaling pathways in macrophages. *Immunobiology* 2006;211: 511–524.
46. Weaver CT, Hatton RD, Mangan PR, Harrington L. E. IL-17 family cytokines and the expanding diversity of effector T cell lineages. *Annu Rev Immunol* 2007;25:821–852.
47. Li MO, Wan YY, Sanjabi S, Robertson AK, Flavell RA. Transforming growth factor-β regulation of immune responses. *Annu Rev Immunol* 2006;24:99–146.
48. Bettelli E, Carrier Y, Gao W, Korn T, Strom TB, Oukka M, Weiner HL, Kuchroo VK. Reciprocal developmental pathways for the generation of pathogenic effector TH17 cells and regulatory T cells. *Nature* 2006; 441:235–238.
49. Huaux F, Lardot C, Arras M, Delos M, Many M-C, Coutelier J-P, Buchet J-P, Renauld J-C, Lison D. Lung firbosis by silica particles in NMRI mice is associated with an up-regulation of the p40 subunit of interleukin-12 and Th-2 manifestations. *Am J Respir Cell Mol Biol* 1999;20:561–572.
50. Sakamoto H, Zhao L-H, Jain F, Kradin R. IL-12p40 −/− mice treated with intratracheal bleomycin exhibit decreased pulmonary inflammation and increased fibrosis. *Exp Mol Pathol* 2002;72:1–9.
51. Dulley FJ, Pennycook AM, Tregoning JS, Hussell T, Openshaw PJ. Differential chemokine expression following respiratory virus infection reflects Th1- or Th2-biasis immunopathology. *J Virol* 2006;80: 4521–4527.
52. Arpinati M, Green CL, Heimfld S, Heuser JE, Anasetti C. Granulocyte-colony stimulating factor mobilizes T helper 2-inducing dendritic cells. *Blood* 2000;95:2482–2490.
53. Dodge IL, Carr MW, Cernada M, Brenner MB. IL-6 production by pulmonary dendritic cells impedes Th1 immune responses. *J Immunol* 2003;170:4457–4464.
54. Gillessen S, Carvajal D, Ling P, Podlaski FJ, Stremlo DL, Familletti PC, Gubler U, Presky DH, Stern AS, Gately MK. Mouse interleukin-12 (IL-12) p40 homodimer: a potent IL-12 antagonist. *Eur J Immunol* 1995;25:200–206.
55. Maynard AD, Baron PA, Foley M, Shvedova AA, Kisin ER, Castranova V. Exposure to carbon nanotube material: aerosol release during the handling of unrefined single-walled carbon nanotube material. *J Toxicol Environ Health A* 2004;67:87–107.